

A Low-Dimensional Learning Model via Convolutional Neural Networks for Unsteady Wake-Body Interaction

T. P. Miyanawala and R. K. Jaiman[†]

Department of Mechanical Engineering, National University Singapore, Singapore 119077

(Received xx; revised xx; accepted xx)

This paper is concerned with the development of a physical model by learning low-dimensional approximation for laminar wake-body interaction systems. Of particular interest is to predict the long time series of unsteady flow dynamics using the learned low-dimensional model. We consider convolutional neural networks (CNN) for the learning dynamics of wake-body interaction, which assemble layers of linear convolutions with nonlinear activations to automatically extract the low-dimensional features. Using high-fidelity time series data from the stabilized finite element Navier-Stokes solver, we first project the dataset to a low-dimensional subspace using proper orthogonal decomposition (POD). The time-dependent coefficients of the POD subspace are mapped to the flow field via a CNN with nonlinear rectification, and the CNN is iteratively trained using the stochastic gradient descent method to predict the POD time coefficient when a new flow field is fed to it. The time-averaged flow field, the POD basis vectors and the trained CNN are used to predict the long time series of the flow fields and results are compared with the full-order (high-dimensional) simulation results. POD-CNN based predictions maintain a remarkable accuracy in the entire fluid domain including the highly nonlinear near wake region for the long time series. The proposed POD-CNN model based on data-driven approximation has a profound impact on the predictive analysis of unsteady wake flow and fluid-structure interaction.

1. Introduction

Development of an efficient model for the prediction and identification of unsteady flow patterns is one of the outstanding challenges in fluid dynamics. Particularly in wake-body interaction systems, predictions of nonlinear phenomena such as the flow separation, the vortex formation, the shear layer and the wake-body synchronization pose a daunting task for the current state-of-the-art analytical tools. Moreover, these complex spatial-temporal characteristics are strongly dependent on physical parameters and geometric variations. While the current computational techniques provide high-fidelity data, they are time-consuming and expensive for long time series extraction. Furthermore, once generated, these high-fidelity data are rarely utilized to increase the efficiency of the subsequent flow field extraction and prediction. Herein, we are interested in the development of a general data-driven low-dimensional model to efficiently forecast the time series of flow fields using the high-dimensional simulation data. During the development of this statistically stationary dynamical model, we surmise that the dominant flow features lie on an embedded nonlinear low-dimensional manifold within the high-dimensional space.

The dimensionality reduction based on proper orthogonal decomposition (POD) provides a low-dimensional data-driven approximation for analyzing dynamical

[†] Email address for correspondence: mperkj@nus.edu

systems Rowley & Dawson (2017). We project a high-fidelity dataset to a low-dimensional subspace whereas POD gives time-invariant spatial modes/basis related to significant physical features such as vortex street, shear layer and near-wake bubble (Miyanawala & Jaiman 2018). This low-dimensional basis is mainly used to reconstruct the already available field and extract the significant flow features which influence the underlying dynamics. One of the recent approaches for handling high-dimensional data is to learn the hidden representation automatically by supervision with the output via neural networks. Machine learning techniques, especially the biologically-inspired (neuron-based) learning, provide the prediction capability required for the flow field generation. In particular, convolution based neural networks with nonlinear rectification known as convolutional neural networks (CNN) have some attractive properties such as local connectivity, nonlinear embedded mapping and parameter sharing. In a recent work of Miyanawala & Jaiman (2017), the authors have demonstrated the ability of CNN for unsteady force prediction along with its physical analogy and justifications for the deterministic analysis of flow dynamics using the Navier-Stokes equation. The present study addresses two fundamental questions: (i) can we utilize POD approximation to learn low-dimensional features for predicting unsteady laminar wake fields? (ii) can we generalize combined POD-CNN for the simulation of wake-body synchronization while assuming the interaction of dominant low-dimensional features with the vibrating bluff body?

In this paper, we combine the POD and CNN techniques in a way to take the advantage of the optimal low-dimensional representation given by POD and the multi-scale feature extraction by the CNN. More specifically, we develop an efficient CNN model which is trained to learn the functional relationship between the present flow field (input) and time-varying POD coefficients of the future time step (output). During the training phase, the CNN is fed with a set of known input-output combinations obtained by the full-order model (FOM). Using the trained CNN, we can feed a known flow field and predict the unknown time coefficients of the next time step. We apply the proposed POD-CNN technique to wake-body interaction systems which have statistically stationary dynamical behavior. We consider a canonical problem of a laminar unsteady wake interacting with an elastically-mounted square cylinder because it offers distinct flow features that are linearly independent and can be learned to predict future flow fields. We assess the predictions of the long time series of flow fields, namely global accuracy of the full domain, local resolution of the non-linear wake regions, the accuracy of the derived statistics such as the fluid forces on the bluff body. Predictions of unsteady wake-body interaction via low-dimensional learning model have a broad range of engineering applications with regard to design optimization, parameter space exploration and the real-time control and monitoring.

2. Low-dimensional learning model

Herein, we present a low-dimensional learning model which is trained using the full-order simulation data to produce the unknown future flow fields efficiently without solving the governing differential equations. While we utilize POD for the low-dimensional approximation, we consider convolutional neural networks as the learning technique, wherein we do not explicitly map adjacent flow fields. To train a CNN explicitly for such high-dimensional many-to-many mapping, there is a need for significantly many convolution layers and/or kernels. When the number of convolution layers is increased and/or larger kernels are used, a weight in the final layer of the CNN represents a very large size problem. In this brute-force manner, the CNN loses the local connectivity which

is essential to capture smaller length scale features present in the unsteady separated flows. Moreover, it makes the CNN extremely less efficient to train and execute for useful predictions. We further assume that the solution space of the unsteady wake system attracts a low-dimensional subspace, which allows building a set of POD basis vectors from the high-dimensional space. We map the time-dependent fluctuations of this low-dimensional representation with the known flow field data to train and predict the unknown flow fields. By combining the dimensional reduction of the POD and the locally-connected learning process of CNN, we next describe our efficient and accurate flow field prediction technique for wake-body interaction systems.

2.1. POD-CNN procedure

The prediction technique requires a high-fidelity series of snapshots of the flow field obtained by full-order simulations, experiments or field measurements. Let $\mathbf{Y} = \{\mathbf{y}_1 \mathbf{y}_2 \dots \mathbf{y}_n\} \in \mathbb{R}^{m \times n}$ be the flow field data set where $\mathbf{y}_i \in \mathbb{R}^m$ is the flow field snapshot at time t_i and n is the number of snapshots. $m \gg n$ is the number of data points, for example, number of probes in an experiment or field measurements or the number of mesh nodes in a numerical simulation. The target is to predict the future flow fields: $\mathbf{y}_{n+1}, \mathbf{y}_{n+2}, \dots$ using the data set \mathbf{Y} . The proposed POD-CNN technique can be divided into four key steps, which are as follows:

Step 1: Generate the proper orthogonal decomposition (POD) basis for data set \mathbf{Y}

Using the n snapshots we can determine the mean field ($\bar{\mathbf{y}} \in \mathbb{R}^m$), the POD modes ($\mathbf{V} \in \mathbb{R}^{m \times k}$) and the time dependent POD coefficients, such that

$$\mathbf{y}_i \approx \bar{\mathbf{y}} + \mathbf{V} \mathbf{A}_i, \quad i = 1, 2, \dots, n \quad (2.1)$$

where $\mathbf{A}_i = [a_{i1} \ a_{i2} \ \dots \ a_{ik}] \in \mathbb{R}^k$ are the time coefficients of the first k significant modes for the time t_i . The vectors $\{\mathbf{A}_1, \mathbf{A}_2, \dots, \mathbf{A}_n\}$ can be determined using the POD reconstruction technique based on linear or nonlinear projections. Note that $k \leq n \ll m$ and k can be estimated via the mode energy distribution. This decomposition reduces the order of the flow field from $O(m)$ to $O(k)$. Now the problem of predicting $\mathbf{y}_{n+1} \in \mathbb{R}^m$ simply reduces to the determination of the matrix $\mathbf{A}_{n+1} \in \mathbb{R}^k$.

Step 2: Train the convolutional neural networks

We employ convolutional neural network described Section in 2.2 as the learning method. The CNN is employed between the flow field data set \mathbf{y}_{i-1} and the POD time coefficients \mathbf{A}_i . We can obtain a mapping using the following functional relationships:

$$\mathbf{A}_i = f(\mathbf{y}_i), \quad \mathbf{y}_i = g(\mathbf{y}_{i-1}), \quad \mathbf{A}_i = f \circ g(\mathbf{y}_{i-1}), \quad (2.2)$$

where f is the mapping between the time coefficients and flow field. For example, in linear POD reconstruction, f is the inner product $\langle \mathbf{y}_i - \bar{\mathbf{y}}, \mathbf{V} \rangle$ and g is the unknown mapping between the flow fields of adjacent time steps. Set the convolutional neural network such that the data set $\{\mathbf{y}_1, \mathbf{y}_2, \dots, \mathbf{y}_{n-1}\}$ is mapped to the POD coefficient set $\{\mathbf{A}_2, \mathbf{A}_3, \dots, \mathbf{A}_n\}$ so that $f \circ g$ map is transformed to

$$\mathbf{A}_i = F(\mathbf{y}_{i-1}, \mathbf{K}, \mathbf{w}), \quad (2.3)$$

where \mathbf{K} and \mathbf{w} are the time-independent trained kernels and weights and F denotes the CNN operation. The CNN is initialized with guessed convolution kernels and weights. It predicts the outputs and compares them with the real output and iteratively adjusts the kernels and weights. Once trained, \mathbf{K} and \mathbf{w} forms an offline network which outputs

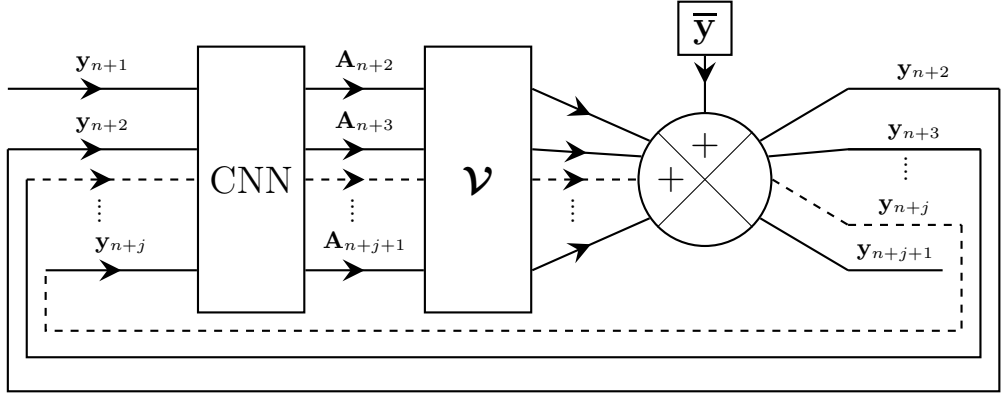


Figure 1: Block diagram for the iterative prediction of the flow fields. The prediction starts from \mathbf{y}_{n+1} and loops until the desired number of time steps are predicted. Here it depicts the prediction of ' j ' number of flow fields from \mathbf{y}_{n+1} to \mathbf{y}_{n+j+1} .

the POD coefficients of the next time step when fed with the flow field matrix.

Step 3: Prediction of \mathbf{A}_{n+1}

In Step 2, note that the known flow field of the last time step, \mathbf{y}_n , is not used for the CNN training. By feeding it to the trained CNN, we can obtain the unknown POD time coefficients at t_{n+1} : \mathbf{A}_{n+1} . Using \mathbf{A}_{n+1} , we can estimate the predicted flow field at t_{n+1} (\mathbf{y}_{n+1}) as follows:

$$\mathbf{y}_{n+1} \approx \bar{\mathbf{y}} + \mathbf{V}\mathbf{A}_{n+1}. \quad (2.4)$$

Step 4: Loop through offline database and predict all other steps

After establishing the above steps, we can utilize the mean, the POD modes and the trained CNN to iteratively predict the future time steps starting from \mathbf{y}_{n+1} . An illustration of the process is shown in figure 1. This technique is capable of predicting any number of time steps provided that an adequate amount of high-fidelity data is used to determine the mean and the POD modes, and to train the CNN properly such that the prediction error is within the acceptable range for the predicted time series. We further elaborate on the integration of POD-based low-dimensional approximation with the CNN process.

2.2. Convolutional Neural Network

The convolutional neural network is designed to map the output and input taking the spatial features of the input into account. First, the CNN is trained using a known dataset and then used for predictions. The training phase consists of iterative predictor (feed-forward) and corrector (back-propagation) processes. Here, we briefly describe the components of the CNN in the context of flow field time series prediction. Refer to Miyanawala & Jaiman (2017) for further elaboration on the use of CNN for fluid mechanics and Goodfellow *et al.* (2016) for CNNs in general. The training phase of the CNN involves the input function, the feed-forward process and the back-propagation process.

Determination of the proper input and output fields is critical for the design of the CNN. For example, it is possible to map the flow fields $\{\mathbf{y}_1, \mathbf{y}_2, \dots, \mathbf{y}_{n-1}\}$ directly to the

flow fields of the adjacent time step $\{\mathbf{y}_2, \mathbf{y}_3, \dots, \mathbf{y}_n\}$. This $m \times n - 1$ to $m \times n - 1$ mapping will require an extremely complex CNN with many layers. The training process will be computationally expensive and time consuming and the network is prone to overfitting and errors. Using POD, we can reduce the order of the output to $k \times n - 1$ such that only the POD time coefficients $\{\mathbf{A}_2, \mathbf{A}_3, \dots, \mathbf{A}_n\}$ are mapped to the flow field. The mean and the POD modes are stored to be used in the predictions. Further, the CNN does not require the refinements and connectivities of a computational fluid dynamics solver mesh. Hence a 2D, uniform, coarse and ordered point-cloud with interpolated fluid field values are used as the input function. In this paper, we use triangulation-based linear interpolation to convert the $\mathbf{Y} \in \mathbb{R}^{m \times n}$ dataset to the tensor $\mathbf{Y}^* = \{\mathbf{y}_1^*, \mathbf{y}_2^*, \dots, \mathbf{y}_n^*\} \in \mathbb{R}^{p \times q \times n}$ where p, q are the spatial dimensions of the 2D point-cloud. Remarkably, the size of \mathbf{y}_i^* is lower than a typical 2D mesh for a laminar DNS simulation and is uniform regardless of the original mesh size. Once the input and output are decided, the CNN iteratively applies the feed-forward (predictor) and back-propagation (corrector) processes until the required convergence is achieved.

The feed-forward process applies the operations: convolution, rectification and down-sampling in sequence, first on the input matrix, then on the output obtained from the above operations. The convolution is a discrete operation which outputs a 3D tensor \mathbf{z}_i^c for each input \mathbf{y}_i^* (Goodfellow *et al.* 2016):

$$\mathbf{z}_i^c = \{z_{i\alpha\beta j}^c\} = \mathbf{y}_i^* \star \mathbf{K} = \left\{ \sum_{b=1}^q \sum_{a=1}^p y_{iab}^* K_{(\alpha-a+1)(\beta-b+1)j} \right\}, \quad j = 1, 2, \dots, n_k, \quad (2.5)$$

where \mathbf{K} is the adaptive time independent kernel tensor, n_k is the number of convolution kernels and typically $\mathbf{z}_i^c \in \mathbb{R}^{p \times q \times n_k}$. The tensor changes slightly if the convolution stride > 1 and any padding used, both of which are not incorporated in this paper. Further elaborations on the effect of non-unit stride and zero-padding can be found in Goodfellow *et al.* (2016). Since convolution is a linear operation, the rectification process is incorporated to introduce nonlinearity to the training: $\mathbf{z}_i^r = \max(\mathbf{0}, \mathbf{z}_i^c)$. In a typical CNN, the rectification is followed by a down-sampling operation. However, in our study, we observe that it deteriorates the flow dynamic results. Usually, the convolution and rectification operations are repeated sequentially with kernel tensors with different sizing. Then the final tensor is stacked to get a vector $\mathbf{z}_i \in \mathbb{R}^s$, where s is the stacked size of the final vector. This vector is then mapped to the output by simple weights:

$$\hat{\mathbf{A}}_i = \mathbf{w} \mathbf{z}_i, \quad (2.6)$$

where $\mathbf{w} \in \mathbb{R}^{k \times s}$ is the adjustable time-independent weight matrix and $\hat{\mathbf{A}}_i$ is the predicted output of the CNN. This mapping is also known as a fully-connected layer. A CNN may contain more than one such fully-connected layers which are not discussed herein. During the training, we calculate the error between the predicted ($\hat{\mathbf{A}}_i$) and true (\mathbf{A}_i) outputs and iteratively adjust the kernel tensors (\mathbf{K}) and weight matrices (\mathbf{w}) using the back-propagation technique.

The training phase of the CNN is an iterative process, which continuously minimizes the error between the predicted and actual outputs. It compares the output of the feed-forward pass with the full-order result and corrects the kernels and weights to minimize the error. For ease of explanation, let us denote these adjustable elements as \mathcal{W} . We define a cost function \mathcal{C} to measure the discrepancy between the feed-forward prediction and full-order POD coefficients:

$$\mathbf{E}_i = \mathcal{C}(\hat{\mathbf{A}}_i, \mathbf{A}_i). \quad (2.7)$$

In this study, the cost function \mathcal{C} is the root mean square error L_2 function. Now the target is to update the weight set \mathbf{W} to minimize the error \mathbf{E}_i using a gradient descent back-propagation method. In what follows is a brief description of the back-propagation.

For simplicity, let us denote the output of the l^{th} layer (sub-routine) of the feed-forward process as \mathbf{z}_i^l . It can be related to the previous layer output $\mathbf{z}^{(l-1)_i}$ and the weights of the l^{th} layer \mathbf{W}^l :

$$\mathbf{z}_i^l = \mathbf{G}(\mathbf{W}^l, \mathbf{z}_i^{l-1}), \quad (2.8)$$

where \mathbf{G} represent a single pass of convolution, rectification and down-sampling (if any) or a fully connected layer. Note that, for an N -layered CNN, $\mathbf{z}_i^0 = \mathbf{y}_i^*$ and $\mathbf{z}_i^N = \hat{\mathbf{A}}_i$. The back-propagation process starts at the predicted value where the error gradient of the fully connected layer can be determined first. When the error gradient of the l^{th} layer: $\frac{\partial \mathbf{E}_i}{\partial \mathbf{z}_i^l}$ is known, we can get the error gradients using the chain rule:

$$\begin{aligned} \frac{\partial \mathbf{E}_i}{\partial \mathbf{W}^l} &= \frac{\partial \mathbf{G}}{\partial \mathbf{W}} (\mathbf{W}^l, \mathbf{z}_i^{l-1}) \frac{\partial \mathbf{E}_i}{\partial \mathbf{z}_i^l}, \\ \frac{\partial \mathbf{E}_i}{\partial \mathbf{z}_i^{l-1}} &= \frac{\partial \mathbf{G}}{\partial \mathbf{z}} (\mathbf{W}^l, \mathbf{z}_i^{l-1}) \frac{\partial \mathbf{E}_i}{\partial \mathbf{z}_i^l}, \end{aligned} \quad (2.9)$$

where $\frac{\partial \mathbf{G}}{\partial \mathbf{W}}$ and $\frac{\partial \mathbf{G}}{\partial \mathbf{z}}$ are the Jacobians of \mathbf{G} relative to \mathbf{W} and \mathbf{z} , and are evaluated at the l^{th} layer. After the evaluation of all the error gradients $\frac{\partial \mathbf{E}_i}{\partial \mathbf{W}^l}$, we use the stochastic gradient descent method with momentum (SGDM) (Rumelhart *et al.* 1988) to adjust the parameter set for the T^{th} iteration:

$$\mathbf{W}_T = \mathbf{W}_{T-1} - \gamma \frac{1}{S} \sum_{p=1}^S \frac{\partial \mathbf{E}_i}{\partial \mathbf{W}} + \psi(\mathbf{W}_{T-1} - \mathbf{W}_{T-2}) \quad (2.10)$$

where $\gamma > 0$ is the learning rate, $\psi \in [0, 1]$ is called the momentum and it is the hyper-parameter which determines the contribution from the previous gradient correction. S is the stochastic sample (mini-batch) size. The gradient in the SGDM is an expectation with a provable convergence, which may be approximately estimated using a small set of samples (LeCun *et al.* 2012). In the next section, we present the effectiveness of the POD-CNN technique for the predictions of flow fields and the wake dynamics behind a freely vibrating square cylinder in cross-flow.

3. Results and discussion

3.1. Problem set-up

In this work, for the first time, we apply a combined proper orthogonal decomposition and convolutional neural network to determine the dynamic fluid fields. We consider a prototypical fluid-structure interaction (FSI) set-up of an elastically-mounted cylinder to extract the unsteady flow field and to predict the coupled dynamical data. In this wake-cylinder problem, the low-dimensional flow structures such as vortex street, the shear layer and the near-wake can be interpreted as an embedded feature into the high-dimensional snapshots. The idea for the POD-CNN model is to extract these low-dimensional features and to predict the dynamic flow fields via the learned low-dimensional model. In particular, we are interested to predict the time-series of the pressure field and the pressure forces on a generic fluid-structure interaction problem. While the proposed technique can be generalized for any fluid-structure system involving the interaction dynamics of flexible structures with an unsteady wake-vortex system, we consider a freely vibrating square cylinder in cross-flow, identical to

Miyanawala & Jaiman (2018). The cylinder is free to oscillate in the streamwise (X) and the transverse (Y) directions. The wake-body synchronization is strongly influenced by the following non-dimensional parameters, namely mass-ratio ($m^* = \frac{M}{m_f}$), Reynolds number ($Re = \frac{\rho^f U_\infty D}{\mu^f}$), reduced velocity ($U_r = \frac{U_\infty}{f_n D}$), and critical damping ratio ($\zeta = \frac{C}{2\sqrt{KM}}$) defined as where M is the mass per unit length of the body, C and K are the damping and stiffness coefficients, respectively for an equivalent spring-mass-damper system of a vibrating structure, U_∞ and D denote the free-stream speed and the diameter of the cylinder, respectively. The natural frequency of the body is given by $f_n = (1/2\pi)\sqrt{K/M}$ and the mass of displaced fluid by the structure is $m_f = \rho^f D^2 L_c$ for a square cross-section, and L_c denotes the span of the cylinder. We particularly select these parameters to represent an FSI system with a low mass and damping ratios and undergoing synchronized wake-body motion. To obtain the high-dimensional approximation of the coupled wake-body interaction using the incompressible Navier-Stokes equations and the rigid body dynamics, we employ the stabilized finite element method and a strongly coupled fluid-structure coupling scheme. Further details of the numerical methodology, the problem set-up and the discretization parameters can be found in Miyanawala & Jaiman (2018).

We perform full-order simulations to extract an adequate number of pressure field snapshots. Using the flow field data, we first calculate the mean field, the POD basis vector and the POD time coefficients. Subsequently, we feed the pressure snapshots and POD coefficients as input-output pairs to the CNN. This allows to obtain long time series of the pressure and velocity fields within the error threshold. Using the pressure field, we evaluate the time history of the pressure-induced drag (C_{Dp}) and lift (C_{Lp}) forces given by:

$$C_{Dp} = \frac{1}{\frac{1}{2}\rho^f U_\infty^2 D} \int_{\Gamma} (\boldsymbol{\sigma}_p \cdot \mathbf{n}) \cdot \mathbf{n}_x \, d\Gamma, \quad C_{Lp} = \frac{1}{\frac{1}{2}\rho^f U_\infty^2 D} \int_{\Gamma} (\boldsymbol{\sigma}_p \cdot \mathbf{n}) \cdot \mathbf{n}_y \, d\Gamma, \quad (3.1)$$

where Γ denotes the fluid-solid interface, $\boldsymbol{\sigma}_p = -p\mathbf{I}$ is the pressure contributed stress component, \mathbf{n}_x and \mathbf{n}_y are the Cartesian components of the unit normal vector \mathbf{n} . We further assess the POD-CNN based predictions with the full-order results in Section 3.3.

3.2. Tuning of the neural network

Extreme refining and overuse of the convolution layers may cause the CNN to overfit the training data set and make it incapable of predicting the flow fields other than the training dataset. However, the under-utilization of convolution will increase the error of prediction. Here, we present an empirical sensitivity study to establish the hyper-parameter values for the best performance of the CNN. Specifically, we address some of the general issues raised by Kutz (2017) for deep learning methods in fluid flows namely, the size of the kernels, the number of kernels per layer, mini-batch size and the learning rate to be used in the CNN. We carry out the FOM on a general laminar wake-body interaction case where the bluff body undergoes significant motion and exhibits statistically stationary flow dynamics. The problem selected here is a square cylinder FSI system with $Re = 125$, $m^* = 3.0$, $U_r = 6.0$ and $\zeta = 0.05$ and we collect ($n = 301$) snapshots. Next, we run the POD-CNN prediction to obtain 300 future pressure fields. To evaluate the trained model, the mean squared error (MSE) is calculated for each prediction which is given by:

$$MSE = \frac{1}{m} \sum_{i=1}^m \left(\hat{P}_i - P_i \right)^2, \quad (3.2)$$

■ POD-CNN ○ FOM

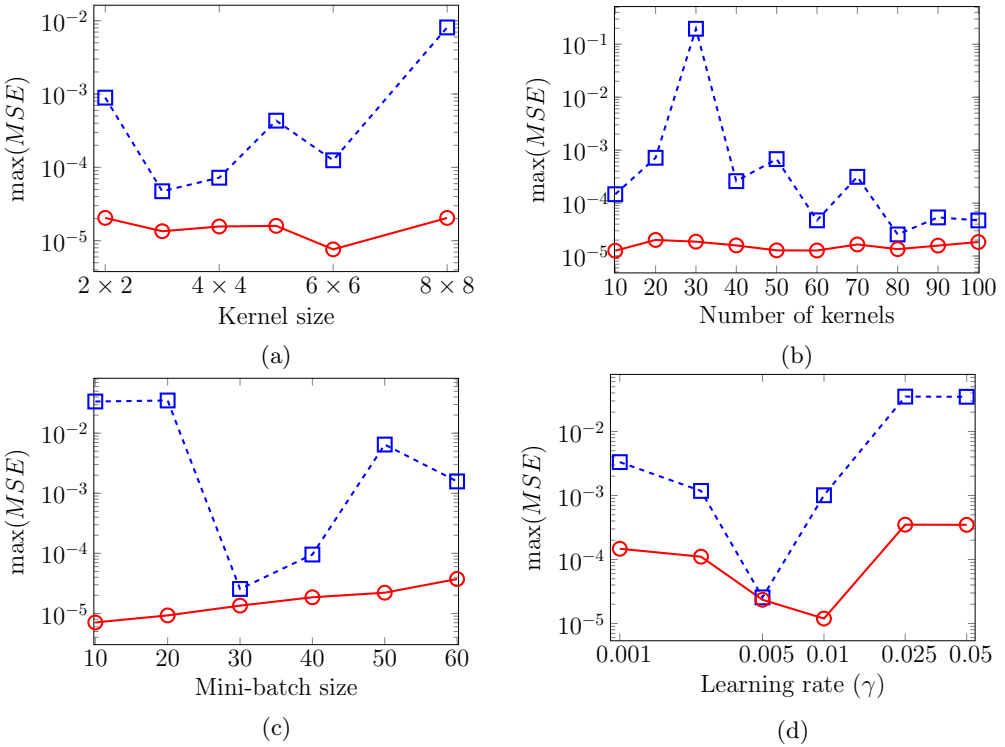


Figure 2: Hyper-parameter tuning for CNN: the trained network is fed, (i) iteratively by the predicted pressure fields and (ii) individually by the FOM pressure fields for comparison. Variation of maximum MSE after 300 predictions against: (a) CNN kernel size (60 kernels, mini-batch size = 30, $\gamma = 0.005$), (b) number of kernels (3×3 kernels, mini-batch size = 30, $\gamma = 0.005$), (c) mini-batch size (80, 3×3 kernels, $\gamma = 0.005$) and (d) learning rate (80, 3×3 kernels, mini-batch size = 30)

where m is the mesh count, \hat{P}_i and P_i are the predicted and true normalized pressure of the i^{th} node of the mesh, respectively. To demonstrate the POD-CNN model, we consider the maximum MSE of the 300 predicted pressure fields for the comparison purpose. Figure 2 summarizes the hyper-parameter optimization for our POD-CNN predictions. We only use one convolution layer, one rectification layer and one fully-connected layer for each POD mode. We assume that, in the convolution layer, 60 kernels have to be used with mini-batch size = 30 and learning rate (γ) = 0.005 and check the best kernel size. Subsequently, we optimize the number of kernels, mini-batch size and the learning rate. Notably, we find that a network with a single convolution layer with 80 kernels of size 3×3 , mini-batch size = 30 and $\gamma = 0.005$ gives the best performance. The pressure field prediction results of this CNN is presented in the next section.

3.3. Pressure field prediction

We first use the convolutional neural network designed in Section 3.2 to extract the time-series of the pressure field of the laminar FSI system: a freely vibrating square cylinder in a uniform flow with $Re = 125$, $m^* = 3.0$, $U_r = 6.0$ and $\zeta = 0.05$. First, we obtain 301 pressure field snapshots (\mathbf{P}_i , $i = 1, 2, \dots, 301$) using the FOM and calculate

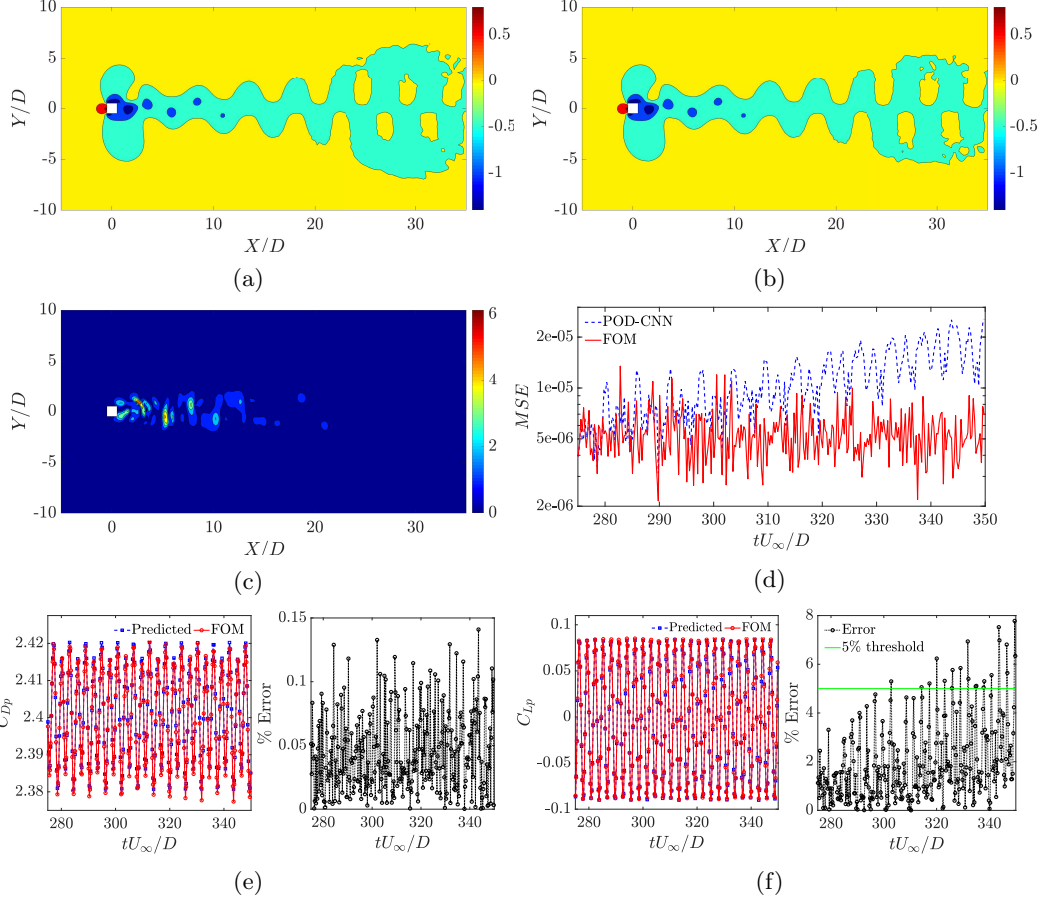


Figure 3: Prediction accuracy of the POD-CNN for a laminar flow at $Re = 125, U_r = 6.0, m^* = 3.0$: (a) predicted, (b) original pressure fields, (c) normalized error of the 300th predicted time step, (d) mean squared error of the first 300 pressure field predictions. Pressure drag (e) and lift prediction (f) and the associated error. Pressure values are normalized by $\frac{1}{2}\rho U_\infty^2$. The flow is from left to right.

the mean ($\bar{\mathbf{P}}$), the POD basis (\mathcal{V}) and the POD coefficients ($\mathbf{A}_i, i = 1, 2, \dots, 301$). After that, we feed the $(\mathbf{P}_i, \mathbf{A}_{i+1}), i = 1, 2, \dots, 300$ pairs to train the CNN. The mean, the POD basis and the trained CNN are then employed to predict the pressure field time series: $\hat{\mathbf{P}}_i, i = 302, 303, \dots, 601$. The predictions are compared against the true pressure field series $\mathbf{P}_i, i = 302, 303, \dots, 601$ obtained by the FOM.

Figure 3 illustrates the prediction quality of the POD-CNN technique. For the first time, we are able to extract the flow field without the use of a full-order simulation and yet maintain a remarkable accuracy. Figure 3(a) and figure 3(b) are the predicted and FOM pressure fields for the 300th time step ($\hat{\mathbf{P}}_{601}$ and \mathbf{P}_{601}). Figure 3(c) displays the percentage error between these two fields, which is below 6.2%. The proposed POD-CNN model maintains the mean-squared errors of the 300 flow fields below 3×10^{-5} (figure 3(d)) hence the POD-CNN model has learned to predict the unsteady flow fields over a broad range of time steps. For comparison, we feed the POD-CNN with the true pressure fields and evaluate the error of the predictions. The error begins to increase

as a function of time, while the MSEs of the predictions are maintained between $[2 \times 10^{-6}, 2 \times 10^{-5}]$. The iterative prediction gives almost the same accuracy for the entire time range. Furthermore, the streamwise (drag) and the cross-flow (lift) forces due to the pressure field are extracted for both POD-CNN and FOM simulations. We have an excellent match between the results (figures 3 (e) and (f)). The pressure drag prediction has an accuracy of 99.8%. Considering the lift force due to the pressure field, all the predictions have a 92% accuracy and 279/300 (93%) of the time steps are above the 95% accuracy threshold. Although a canonical laminar flow of vibrating square is considered, the present POD-CNN learning technique does not make any assumptions with regard to geometry and boundary conditions.

4. Concluding remarks

We have presented a novel low-dimensional learning model based on the POD and CNN approximations for unsteady wake flows and wake-body interaction. While the POD provides an optimal extraction of dominant flow features, the CNN enables nonlinear correlation of fluid motions to construct time-series of flow field using the trained neural networks. We successfully demonstrated the effectiveness of the proposed technique by predicting the time series of the unsteady pressure field of an FSI set-up of an elastically-mounted square cylinder. We tuned the hyper-parameters: number of kernels, kernel size, training batch size and learning rate of the CNN to provide most accurate predictions. For the first time, using the low-dimensional approximation and the CNN-based learning, we are able to predict the flow patterns of a long time series using the same full-order mesh with reasonable accuracy. The quantities derived from the flow fields such as the pressure drag and lift were also accurately predicted. The present low-dimensional learning technique can be implemented using only a fraction of computational resources to that of FOM and allows rapid exploration of flow pattern variations due to the design parameter variations (e.g., bluff body geometry and structural parameters).

The first author thanks the Ministry of Education, Singapore for the financial support.

REFERENCES

GOODFELLOW, I., BENGIO, Y. & COURVILLE, A. 2016 *Deep learning*, , vol. 1. Cambridge: MIT press.

KUTZ, J. N. 2017 Deep learning in fluid dynamics. *Journal of Fluid Mechanics* **814**, 1–4.

LECUN, Y. A., BOTTOU, L., ORR, G. B. & MÜLLER, K. R. 2012 Efficient backprop. In *Neural networks: Tricks of the trade*, pp. 9–48. Springer.

MIYANAWALA, T. P. & JAUMAN, R. K. 2017 An efficient deep learning technique for the Navier-Stokes equations: Application to unsteady wake flow dynamics. *arXiv preprint arXiv:1710.09099* .

MIYANAWALA, T. P. & JAUMAN, R. K. 2018 Decomposition of wake dynamics in fluid-structure interaction via low-dimensional models. *arXiv preprint arXiv:1806.00396* .

ROWLEY, C. W. & DAWSON, S. T. M. 2017 Model reduction for flow analysis and control. *Annual Review of Fluid Mechanics* **49**, 387–417.

RUMELHART, D. E., HINTON, G. E. & WILLIAMS, R. J. 1988 Learning representations by back-propagating errors. *Cognitive modeling* **5** (3), 1.